Media Synchronization in ATM Network-based Distributed Multimedia Systems

Ying Hao and Jyh–Charn Liu
Department of Computer Science
Texas A&M University
College Station, TX 77843–3112

Abstract

This paper exploits the impact of the Asynchronous Transfer Mode (ATM) transport standard on the mutual synchronization of multiple media servers in a distributed multimedia system. On the basis of a bursty traffic model, we develop and analyze an effective media synchronization scheme. In our scheme the media terminal (MT), which receives continuous streams of data from different media servers, acts as the coordinator for mutual synchronization of the media servers. The correlation between the time skew of clocks in the media servers and the network transmission behavior is analyzed, with the bursty traffic of the ATM network taken into account. We quantify the correlation between the resynchronization time interval, the clock drift rate, the time skew of servers, and the the network jitter. Our results suggest that in allocation of ATM network resources to virtual channels (VC), the transmission delay, cell loss probability and synchronization of clocks are equally important in distributed multimedia systems.

1 Introduction

Distributed multimedia systems represent one of the most challenging applications to the computer and communication industry. Geographically distributed media servers (MAS) with high storage capacities can provide a user with different types of information on one *media terminal* (MT), which can be a workstation equipped with high-fidelity speakers or other display devices. In a distributed multimedia system, several MASes may provide an MT simultaneously with information in different media formats continuously (video, audio) or sporadically (image, text). For different information sources with significant temporal correlations, it is important to keep them synchronized to each other within a reasonable time bound. Otherwise, it may cause disturbing visual or sound effects to the users. A common technique to solve this problem is through mutual synchronization of the output rates of MASes [1, 2, 3]. For example, media synchronization requirements are formalized in [1]. An adaptive feedback media synchronization scheme is proposed in [4], in which the network is assumed to have bounded delays, so that we can obtain the bounds on the time skew of logical clocks.

Three factors contribute to media asynchrony, which is the time skew between different medias in an MT: the network delay jitter, media transmission rates, and the initialization phase difference, of MASes. The network delay jitter is caused by nondeterministic cell transmission delays. If a large transmission delay jitter exists between different communication paths, then temporary loss of synchrony between continuous media objects may be observed. Drifting rates of clocks in MASes can be compensated for by periodic adjustment of their clocks to synchronize their media retrieving rates within an acceptable range. For simplicity, we assume that the initialization phase difference is eliminated when the connections are established, and we concentrate on the other two factors in this paper.

A high speed network is a vital element of a distributed multimedia information system [1, 2, 5, 6] for transporting large volumes of data between distant sites. The *Asynchronous Transfer Mode (ATM)* which operates on a high speed fiber optical transmission system is one of the most promising transport standards to support multimedia applications [7]. An ATM network operates in a packet switched, connection-oriented mode, in which each packet, called a *cell*, is 53 bytes long. A broadband ATM network can accommodate a wide range of multimedia information including text, pictures and video/audio signals, etc., using a single communication standard. In an ATM network, two users communicate with each other through one or more fixed routes called virtual channels (VC) to exchange information. A VC between two users needs to be established first before actual information exchange can take place. If two VCs traverse the same communication link, they will be statistically multiplexed to share the link bandwidth. Therefore, when data streams from different media servers are transmitted in the same ATM network, the mutual interference between VCs need to be taken into account to meet their communication requirements.

The ATM network is a lossy transmission system, in which excess cells are discarded when the buffer of an ATM switch is full. To meet the service requirements of users without causing network congestion, *resource allocation* and *usage parameter control* (UPC) [8, 9, 10, 11, 12, 13] are the two major mechanisms for preventive congestion control. A resource allocation scheme [14, 15, 16] determines acceptance of new

1063-6927/94 $03.00

connection requests according to their declared traffic characteristics, GOS requirements, and the current network workload. A UPC unit enforces the traffic stream of an information source to conform to its declared characteristics at the edge of the network.

In this paper, we study the impact of the ATM network behavior on mutual synchronization of media servers. We first develop a model to determine the network delay jitter between multiple VCs from different MASes to an MT. We then develop a clock synchronization scheme to control the clock skew between two MASes, with the bursty traffic behavior of the ATM network taken into account. The distributions of the media synchronization anomalies are quantified through analytical models and simulations.

We organize the rest of this paper as follows. We analyze in Section 2 the characteristics of ATM networks which are critically related to the mutual synchronization of multiple MASes. The clock synchronization algorithm and its analysis are discussed in section 3, and analytical and simulation results are given in section 4. Section 5 concludes this paper.

2 Transmission Characteristics of ATM Networks

In our system model, an MT can retrieve continuous media information from any of the MASes. The retrieving rate of the continuous media information from an MAS can be adjusted arbitrarily, based on the request sent by the user at an MT, e.g., fast forward/backward, slow play, freeze, etc. Since the media streams can be edited together to form new, mixed media information, e.g., the video editing capability, the temporal relations between the media information from different MASes can be critical.

In an ATM switch, cells are scheduled by the statistical multiplexing technique. ATM switches are assumed to have an output-buffered, non-blocking switching fabrics architecture, and a buffer is associated with each output port. The buffer space at an output port is globally shared by all the VCs that traverse the output port, and newly arrived cells are discarded when the buffer is full. To avoid accumulation of bursty traffic in the switch, a non-work-conserving, flow regulation mechanism such as the *virtual clock* [17] or the peak rate enforcement scheme [18, 19], is assumed to be used for scheduling of cells at each output port. Cells belonging to the same VC are transmitted based on the first come first serve scheduling scheme.

To model the bursty traffic behavior in an ATM network, the cell stream generated from each MAS is assumed to follow the two-state Modulated Markovian Process (MMP) with states of "on (busy)" and "off (idle)" [9, 20]. The sojourn times of both "on" and "off" states follow exponential distributions, and the interarrival time of cells in each burst is governed by an exponential distribution. In this way, the multiplexed traffic streams from different sources form a multi-state MMP process, in which each state denotes a unique number of sources that are simultaneously active (transmitting cells).

In order to establish a VC, a connection request is made to the network based on the following parameters: 1) its peak cell generation rate λ, 2) the average duration of on-state (or burst length) T_b, 3) the burstiness, which is defined as the ratio between peak and mean cell generation rate of the source [21], and 4) the maximum cell loss probability ψ and maximum cell transmission delay θ. Let $\bar{\lambda}$ denote the average cell generation rate from a source, its burstiness can be calculated as $\lambda/\bar{\lambda}$, and it is clear that $\lambda/\bar{\lambda} = \frac{T_s+T_b}{T_b}$, where T_s is the average duration of the silence period of the source. If the admission control scheme determines that the GOS requirements of both the new and existing VCs and the inter-VC jitter requirement can be satisfied, then the new connection will be granted. Otherwise, the connection should be rejected. We assume that the traffic stream on an established VC conforms to its declared characteristics by a UPC mechanism in its MAS.

Mutual synchronization of media output rates of the two MASes is critically dependent on the transmission quality of the ATM network. For simplicity, our discussion focuses on the control of delay jitter between two VCs in this paper, and our results can be generated for an arbitrary number of VCs. Here, we use a model to estimate the transmission delay jitter between the two MASes. Let D_1 and D_2 be cell transmission delays along the two VCs. $D_1 = \sigma_{10} + S_1$ and $D_2 = \sigma_{20} + S_2$, respectively, where σ_{10} and σ_{20} denote the propagation delay on the two VCs, and S_1 and S_2 denote the queuing delay along the two VCs. Let the cell delay of VC_i be denoted as $f_i(t)$, and the average cell delay of the VC be denoted as $\overline{T_i}$. The delay jitter between cells from the two VCs can be denoted by a random variable $Y = |(d_1 - \overline{S}_1) - (d_2 - \overline{S}_2)|$, and the inter-$VC$ delay jitter between the two VCs can be expressed as

$$J_{12} = \int_{d_1=0}^{\infty} \int_{d_2=0}^{\infty} |(d_1 - \overline{S}_1) - (d_2 - \overline{S}_2)| f_{S_1}(d_1) f_{S_2}(d_2) \mathrm{d}d_1 \mathrm{d}d_2, \quad (1)$$

where $\overline{S}_1$ and $\overline{S}_2$ are mean values of S_1 and S_2, respectively. The density function of the inter-VC jitter can be expressed as

$$f_{J_{12}}(j) = \int_{j=|(d_1-\overline{S}_1)-(d_2-\overline{S}_2)|} f_{S_1}(d_1) f_{S_2}(d_2) \mathrm{d}d_1 \mathrm{d}d_2.$$

It is evident that $f_{J_{12}}(j)$ is dependent on traffic characteristics, and we are particularly interested in the case when the ATM network is loaded with bursty traffic. Without loss of generality, we omit the subscript of S_i and d_i in our subsequent discussion. We note that a precise model on $f_S(d)$ is prohibitively complicated, and thus an approximation model needs to be used for its analysis. To avoid the prohibitively high complexity of an exact model of a bursty ATM network, we have proposed an approximation model called the *cyclic loss model* for characterization of a bursty network [22]. In this model, the cell transmission process in a burst period is approximated by a fluid flow with rate λ. The bandwidth and buffer assigned to the VC are denoted as μ and q, respectively. The source of the VC is assumed to have a peak rate λ, an average on-duration T_b and an average off-duration T_s. When $\lambda \leq \mu$, no cell will be lost. However, when $\lambda > \mu$, cells accumulate in the buffer of the VC at rate $\lambda - \mu$ in on-period. The accumulated cells, if any, will be discharged during the off-period at the discharge rate μ. Therefore, arrivals/departures of bursts can be viewed as a recurrent process, in which the arriving or departing time of each burst can be viewed as a renewal point [22], as shown in Figure 1 (a).

Let B and S denote durations of the on- and off-period of a bursty source, respectively, and their density functions are denoted as $f_B(b)$ and $f_S(s)$. A cycle starts at the beginning of an on-period at time instant t_a, and it ends at time instant t_c, which is the end of the off-period. At t_b ($t_a < t_b < t_c$), the on-period ends and the off-period begins. Since both t_a and t_c are recurrent points, the states of the VC at t_a and t_c are statistically identical. In [22], we solved the $R(\mu, q)$, cell loss probability, and $D(\mu, q)$, delay bound, by deriving the distributions of the queue lengths at t_a, t_b and t_c. We get the delay bound for given bandwidth μ and buffer size q at an output port of a switch [22] as $D(\mu, q) = q/\mu$, and the cell loss probability [16] as

$$R(\mu, q) = \frac{(\lambda - \mu)\gamma}{\lambda} e^{-(\alpha-\beta)q}, \qquad (2)$$

where $\alpha = \frac{1}{(\lambda-\mu)T_b}$, $\beta = \frac{1}{\mu T_s}$, and $\gamma = \frac{\alpha-\beta}{\alpha-\beta e^{-(\alpha-\beta)q}}$. We also get the density function of buffer occupancy at the beginning of a cycle as $f_X(x) = \gamma(\delta(x) + \beta e^{-(\alpha-\beta)t})$. The results mentioned above need to be used to derive $f_S(d)$.

To derive the delay jitter, we need to derive the probability of the cell delay S exceeding a given time bound d, $P_S(S > d)$. Since the average service time of each cell is $\frac{1}{\mu}$, therefore, $P_S(S > d)$ is also equal to the probability of the number of buffered cells N greater than μd, or $P_S(S > d) = P_N(N > \mu d)$. Therefore, we will derive $P_S(S > d)$ by solving the average time period T_d in which the number of buffered cells is greater than μd.

Referring to Figure 2, where X denotes the number of buffered cells at the beginning of a new burst period, and q, ($q \geq \mu d$), denotes the buffer space assigned to the VC. The number of buffered cells can become greater than μd for both $X > \mu d$ or $X \leq \mu d$, as shown in Figure 2 (a) and (b), respectively. If $X \geq \mu d$, then based on the commonly adopted assumption that the service rate (μ) of the VC is smaller than the peak arrival rate (λ) of cells [23], every cell arrived in the on-period will have a delay time of greater than d, implying that $T_d = T_b$. For the case of $X < \mu d$, the cell delay begins to exceed d after a time interval of $\frac{\mu d - x}{\lambda - \mu}$, and we have

$$\begin{aligned} T_d &= \int_{\frac{\mu d - x}{\lambda-\mu}}^{\infty} t f_{T_b}(t) dt \\ &= \int_{\frac{\mu d - x}{\lambda-\mu}}^{\infty} t \frac{1}{T_b} e^{\frac{-t}{T_b}} dt, \text{ if } X < \mu d. \end{aligned}$$

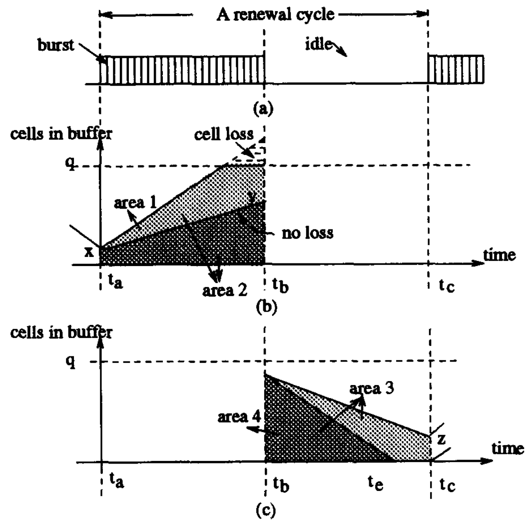

Figure 1: Different growth and shrinkage conditions of the output queue for a VC [22]

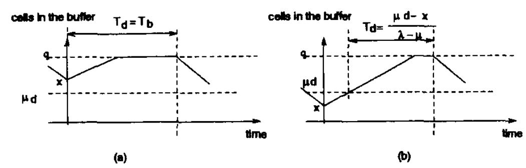

Figure 2: Analysis on the transmission delay distribution (a) $X > \mu d$ and (b) $X \leq \mu d$

By combining the expressions of T_d for conditions $X \geq \mu d$ and $X < \mu d$, we get

$$\begin{aligned} T_d &= \int_{\mu d}^{q} f_X(x) dx T_b + \int_0^{\mu d} f_X(x) \int_{\frac{\mu d - x}{\lambda-\mu}}^{\infty} t f_{T_b}(t) dt dx \\ &= \int_{\mu d}^{q} \gamma(\delta(x) + \beta e^{-(\alpha-\beta)x}) dx T_b \\ &+ \int_0^{\mu d} \int_{\frac{\mu d - x}{\lambda-\mu}}^{\infty} \gamma(\delta(x) + \beta e^{-(\alpha-\beta)x}) t \frac{1}{T_b} e^{\frac{-t}{T_b}} dt dx \\ &= \gamma T_b (\frac{\beta}{\alpha-\beta}(e^{-(\alpha-\beta)\mu d} - e^{-(\alpha-\beta)q}) T_b \\ &+ e^{-\alpha\mu d}((1 + \frac{\alpha}{\beta}) e^{\beta\mu d} - \frac{\alpha}{\beta})). \qquad (3) \end{aligned}$$

Cells arrived during T_d will experience a delay time which is greater than d. However, some of the cells arrived during T_d may be lost. Therefore, we need to exclude those lost cells in derivation of the proportion of cells whose delay exceeds d. The cell loss period T_o in a cycle can be directly derived from (3) by letting $\mu d = q$, as

$$T_o = \int_0^q \int_{\frac{q-x}{\lambda-\mu}}^{\infty} \gamma(\delta(x) + \beta e^{-(\alpha-\beta)x})t \frac{1}{T_b} e^{\frac{-t}{T_b}} dt dx = \gamma T_b e^{-\alpha q}((1 + \frac{\alpha}{\beta})e^{\beta q} - \frac{\alpha}{\beta}). \quad (4)$$

After we get T_d and T_o, the probability of the cell delay exceeding d, $P_S(S > d)$, can be expressed as

$$P_S(S > d) = \begin{cases} \frac{\lambda T_d - (\lambda-\mu)T_o}{\lambda T_b - (\lambda-\mu)T_o} & d < q/\mu \\ 0 & \text{otherwise.} \end{cases} \quad (5)$$

We can thus obtain the density function $f_S^s(d)$ as

$$\begin{aligned} f_S^s(d) &= -P_S'(S > d) \\ &= \frac{\gamma \lambda \mu \alpha^2 (e^{-(\alpha-\beta)\mu d} - e^{-\alpha \mu d}) U(d - q/\mu)}{\beta(\lambda - \gamma(\lambda-\mu)e^{-\alpha q}((1+\frac{\alpha}{\beta})e^{\beta q} - \frac{\alpha}{\beta}))} \\ &+ \frac{\gamma \mu e^{-\alpha q}((1+\frac{\alpha}{\beta})e^{\beta q} - \frac{\alpha}{\beta})\delta(d - q/\mu)}{(\lambda - \gamma(\lambda-\mu)e^{-\alpha q}((1+\frac{\alpha}{\beta})e^{\beta q} - \frac{\alpha}{\beta}))}, \end{aligned} \quad (6)$$

where $P_S'(S > d)$ denotes the differentiation of $P_S(S > d)$, and $\delta(t)$ and $U(t)$ are the impulse and step functions, respectively. The probability distribution on the end-to-end delay can thus be obtained as

$$f_S(d) = \overbrace{f_S^s(d) * f_S^s(d) * \cdots f_S^s(d)}^{k}, \quad (7)$$

where k is the number of switches that the VC passes. We can thus calculate the inter-VC jitter by plugging Equation 7 into Equation 1.

3 Media Synchronization

The synchrony of information flows from MASes is affected by the network delay jitter, and the clock drifting rates of the MASes. We assume that the logical clock in an MAS is linearly scaled to determine the media output rate. Thus the media synchronization problem can be directly modeled as a clock synchronization problem. In reality adjustment to logical clock rates can be done through pausing and skipping of media objects. That is, if the logical clock of an MAS becomes too fast, then transmission of the media objects will be paused. If the clock of an MAS is too slow, then the media output rate of the MAS will be increased by skipping some pieces of the objects [3]. We assume that both clock-synchronization cells and data cells from an MAS is sent to the MT through the same VC, implying that the delay distribution of synchronization and data messages are identical. On the other hand, since only a few cells need to be sent from the MT to its MASes, we assume that the variance of transmission delays from the MT to its MASes are negligible. The transmission delay from the MT to its MASes is assumed to be attained when their VCs are established.

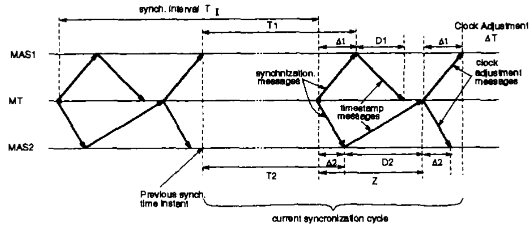

Figure 3: Interactions between nodes during synchronization

The master-slave model is adopted for synchronization of the (local) clocks of MAS_1 and MAS_2. The logical clock of MAS_2 is defined as the master clock, and the logical clock of MAS_1 is adjusted periodically such that the time skew between their clock values can be controlled within a required bound. Let the drift rate of the slave clock with respect to the master clock be denoted as ρ. The slave clock is faster the master clock when $\rho > 0$, otherwise the it is slower than the master clock. The clock of MT need not be synchronized with the clock of neither MASes.

The clock synchronization algorithm works as follows. The MT broadcasts a ***synchronization*** message to the two MASes after a fixed (logical) time interval, called the ***synchronization interval.*** Immediately after receiving the synchronization message, each MAS sends a ***time-stamped message*** to the MT containing its current local time at which the MAS receives the synchronization message. Once the MT receives the time-stamped message from both MASes, it calculates the difference of the two logical clock values and predicts the clock adjustment value ΔT for the two MASes. Then the MT immediately sends a ***clock-adjustment message*** to both MASes. The master MAS only remembers the starting time of the next synchronization cycle without changing its clock value, but the slave MAS immediately adjusts its clock value based on the clock-adjustment message.

The key design parameters which need to be determined for our synchronization algorithm include 1) maximum (clock) synchronization interval, 2) the allocated network resources for inter-VC jitter control, and 3) the clock adjustment value ΔT for the slave MAS. These parameters are related to the network delay, the permissible clock skew for the two MASes, and the clock drift rate. To derive these parameters, we shall first characterize the correlation between adjustments of the slave clock values and the synchronization interval T_I. Then, for a given permissible time skew of the two clocks, we shall derive the relation between the synchronization interval and the clock drift rate, with the network delay taken into account. Finally, we shall derive the probability distribution of clock skew after each adjustment.

The interaction between nodes for inter-MAS synchronization is plotted in Figure 3. Although the communication patterns plotted in Figure 3 show that the transmission time from MAS_2 to MT is longer than the transmission time from MAS_1 to MT, our subsequent discussion does not make any assumptions on the difference between the transmission times of the VCs. The network delays for transmission of the synchronization message from MT to the two MASes are denoted as Δ_1 and Δ_2, respectively, and they are measured in terms of the master clock. Let T_i ($i = 1, 2$) denote time interval from the time instant that MAS_1 set its local clock value in the previous cycle to the time instant that the time-stamped message of MAS_i is generated. T_i is measured in terms of the local clock of MAS_i. T_1 and T_2 are send back to the MT in the time-stamped messages.

Let the transmission delays of the time-stamped messages from the two MASes to the MT be respectively denoted by D_1 and D_2, both of which are measured in terms of the master clock. D_1 (D_2) consists of the link propagation delay and the queuing delay in network switches. Assuming that the link propagation delay is invariant with time, only the switch queuing delay would affect the maximum adjustment interval and the maximum value of the clock skews. After the MT receives the time-stamped messages from both MASes, it calculates their difference as $A = T_1 - T_2$. Now we derive the relation among T_1, T_2 and ρ. Referring to Figure 3, since Δ_1 is measured in terms of master clock and the relative progression rate between clocks of MAS_1 and MAS_2 is $1 + \rho$, the time interval between the time when MAS_1 set its clock in the previous cycle and the time when a synchronization message is sent in the current cycle can be expressed by $T_1 - (1+\rho)\Delta_1$ in terms of the clock rate of MAS_1. Since the same time interval can also be expressed by $T_2 - \Delta_2$ in terms of the clock of MAS_2, the following relation holds:

$$T_1 - (1+\rho)\Delta_1 = (T_2 - \Delta_2)(1+\rho). \tag{8}$$

Hence, ρ can be calculated from Equation 8 as

$$\rho = \frac{T_1 - T_2 - (\Delta_1 - \Delta_2)}{T_2 + (\Delta_1 - \Delta_2)}. \tag{9}$$

Assuming that the MT sends out the two synchronization messages simultaneously. Then, the difference in the clock values of MAS_1 and MAS_2, when MAS_1 receives the synchronization message, is

$$T_S = T_1 - T_2 - (\Delta_1 - \Delta_2). \tag{10}$$

Hence, MAS_1 would be perfectly synchronized if we could subtract T_S from T_1 at the time instant when MT sends the synchronization messages. However, to calculate the clock adjustment value at the time instant that the clock-adjustment message is received by MAS_1, the MT needs to take into account T_S, transmission delays of both the time-stamped messages from MASes and the clock-adjustment message to MASes, and clock skews associated to both transmission delays. The time skew of the two clocks during transmission of the clock-adjustment message is simply $\rho\Delta_1$. The time skew of these two clocks during transmission of the time-stamped messages is $\rho(\max\{D_1 + \Delta_1, D_2 + \Delta_2\} - \Delta_1)$, where $\max\{D_1 + \Delta_1, D_2 + \Delta_2\}$ represents the time interval from the instant that MT sends out the synchronization messages, to the instant that MT receives both time-stamped messages, and the last term Δ_1 reflects the fact that that the time skew between the two clocks during transmission of the synchronization message to MAS_1 has been counted in T_S. Therefore, the amount of clock skew at the instant that MAS_1 receives the clock-adjustment message (***synchronization-point***) can be expressed as

$$\begin{aligned}\Delta T &= T_S + \rho\Delta_1 + \rho(\max\{\Delta 2 + D_1, \Delta_2 + D_2\} - \Delta_1) \\ &= A - (\Delta_1 - \Delta_2) + \rho \max\{D_1 + \Delta_1, D_2 + \Delta_2\},\end{aligned} \tag{11}$$

where $A = T_1 - T_2$ can be calculated by the MT. Let $Z = \max\{D_1 + \Delta_1, D_2 + \Delta_2\}$. Since it is impossible to get the current value of cell delays, we use the mean value of Z, denoted as $\overline{Z}$, instead of Z, for derivation of clock adjustment ΔT. That is, the clock adjustment at the synchronization-point is calculated as

$$\overline{\Delta T} = A - (\Delta_1 - \Delta_2) + \rho\overline{Z}.$$

We now calculate $\overline{Z}$. Since $D_i = S_i + \sigma_{i0}$ ($i = 1, 2$) where σ_{i0} is the propagation delay from MAS_i to the MT and $\Delta_i = \sigma_{0i}$ from our assumption, we can rewrite Z as $Z = \max\{S_1 + \sigma_{10} + \sigma_{01}, S_2 + \sigma_{20} + \sigma_{02}\}$. Since the probability distribution functions of S_1 and S_2 can be obtained from Equation 7 as $P_{S_1}(S_1 < d_1)$ and $P_{S_2}(S_2 < d_2)$, respectively, the probability distribution function of Z can be expressed as $P_Z(Z < t) = P_{S_1}(S_1 < t - (\sigma_{10} + \sigma_{01}))P_{S_2}(S_2 < t - (\sigma_{20} + \sigma_{02}))$. Since S_i is bounded by q_i/μ_i ($i = 1, 2$), Z is also bounded by $B(Z) = \max\{q_1/\mu_1 + \sigma_{10} - \sigma_{01}, q_2/\mu_2 + \sigma_{20} - \sigma_{02}\}$. Thus, we have

$$\overline{Z} = \int_0^{B(Z)} (1 - P_Z(Z < t))dt.$$

After a synchronization activity completes, the clock skew between MAS_1 and MAS_2 may not be zero because of the non-deterministic cell transmission delay in the network. Let S_r denote the remaining clock skew after the current adjustment, which can be calculated as the difference between the real clock skew ΔT and our clock adjustment value $\overline{\Delta T}$. That is,

$$S_r = \Delta T - \overline{\Delta T} = \rho(Z - \overline{Z}). \tag{12}$$

Let S_w denote the clock skew at the time instant immediately before the synchronization point. In the steady state, we have $S_w = S_r + \Delta T$.

We now calculate the maximum synchronization interval for a given permissible clock skew ξ such that $|S_w| < \xi$. From Equations 8 and 10, we have $A = \rho T_2 + (1+\rho)(\Delta_1 - \Delta_2)$. Replacing A in Equation 11, we get

$$\begin{aligned}\Delta T &= \rho T_2 + (1+\rho)(\Delta_1 - \Delta_2) - (\Delta_1 - \Delta_2) + \rho Z \\ &= \rho T_2 + \rho(\Delta_1 - \Delta_2) + \rho Z\end{aligned} \tag{13}$$

Since we know

$$\begin{aligned} |S_w| &= |S_r + \Delta T| \leq |B(S_r)| + |B(\Delta T)| \\ &\leq |\rho(B(Z) - \overline{Z})| + |\rho T_2 + \rho(\Delta_1 - \Delta_2) + \rho Z| \\ &\leq |\rho|(2B(Z) - \overline{Z} + T_2 + |\Delta_1 - \Delta_2|), \quad (14) \end{aligned}$$

the maximum clock skew before the synchronization point can thus be expressed as $|\rho|(2B(Z) - \overline{Z} + T_2 + |\Delta_1 - \Delta_2|)$, which must be smaller than or equal to the permissible skew ξ. Hence we have

$$T_2 \leq \frac{\xi}{|\rho|} - (2B(Z) - \overline{Z}) - |\Delta_1 - \Delta_2| = T_2^*. \quad (15)$$

From Figure 3, we know the relation between the synchronization interval T_I and T_2 as $T_I = T_2 + (\Delta_1 - \Delta_2) + \Delta_1 + Z$. Moreover, since $T_I \leq T_2 + |\Delta_1 - \Delta_2| + B(Z) + \Delta_1 \leq \frac{\xi}{|\rho|} - (B(Z) - \overline{Z}) + \Delta_1$, we get the maximum synchronization interval as

$$T_I^* = \leq \frac{\xi}{|\rho|} - (B(Z) - \overline{Z}) + \Delta_1.$$

After we derive the maximum synchronization interval, we next calculate the probability distribution of clock skew S_w immediately before the synchronization point. Since $S_w = S_r + \Delta T$, and we have S_r and ΔT from equations 12 and 13, respectively, we get

$$\begin{aligned} S_w &= \rho T_2^* + \rho(\Delta_1 - \Delta_2) + \rho(2Z - \overline{Z}) \\ &= 2\rho Z + \rho(T_2^* + (\Delta_1 - \Delta_2) - \overline{Z}). \quad (16) \end{aligned}$$

Therefore,

$$Prob(S_w < t) = Prob(Z < \frac{\rho(T_2^* + (\Delta_1 - \Delta_2) - \overline{Z})}{2}).$$

4 Discussions

In this section, we use an example to illustrate the behavior of the media synchronization algorithm. The traffic characteristics and the GOS requirements of the two VCs to transmit the media information are listed in Table 1. Our example only considers one intermediate ATM switch, but the results can be easily generalized to multiple switches. The propagation delays from MAS_1 and MAS_2 to the MT are assumed to be $\sigma_{10} = 2\ ms$ and $1\ ms$, respectively. By solving $D(\mu_i, q_i) \leq \theta_i$ and $R(\mu_i, q_i) < \psi_i$ for $i = 1, 2$ we calculate the minimum resources (bandwidth and buffer space) allocated to VC_1 and VC_2 as $\mu_1 = 44399bps$ and $q_1 = 10cells$, and $\mu_2 = 376199bps$ and $q_2 = 26cells$, respectively. The transmission delays from the MT to the two MASes are assumed to be $\Delta_1 = 2\ ms$ and $\Delta_2 = 1\ ms$, respectively.

We first show in Figure 4 the accuracy of our model by comparing the inter-VC jitter obtained from our model and simulation. In this case, we fix the amount of resources allocated to MAS_2 but vary the amount of resources allocated to MAS_1. It can be seen that

	GOS		Traffic Characteristics		
MAS	ψ	θ (sec.)	λ (bps)	T_b (ms)	T_s (ms)
1	0.0001	0.1	50000	100	150
2	0.0030	0.03	400000	150	200

Table 1: The traffic characteristics and GOS requirements of the sources

the analytical and simulation results are quite consistent with each other for different amount of resource allocated to MAS_1. It is also shown in Figure 4 that the inter-VC jitter decreases with the amount of bandwidth assigned to the VCs. It should be noted that the abrupt jumps at some points of the curves are caused by the discontinuity of the probability distribution in cell transmission delay because of finite buffer sizes, as dictated in Equation 5.

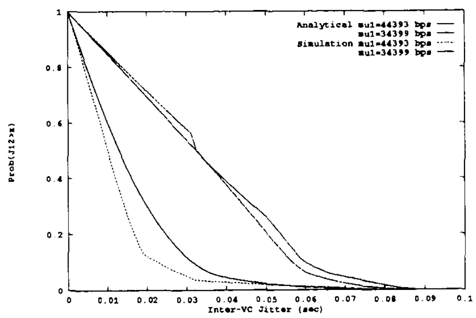

Figure 4: Comparison between analytical and simulated results for MAS_1, where $q_1 = 10cells$

Now, we show in Figure 5 the clock skew at the time instant immediately before synchronization-point, at which the largest clock skew would be observed. We plot in the figures the probability that the clock skew is greater than a given value in the X-axis. The four different diagrams reflect the clock skew behavior when exactly one of the allocated resources to the two VCs varies. We can see that resource allocations can have

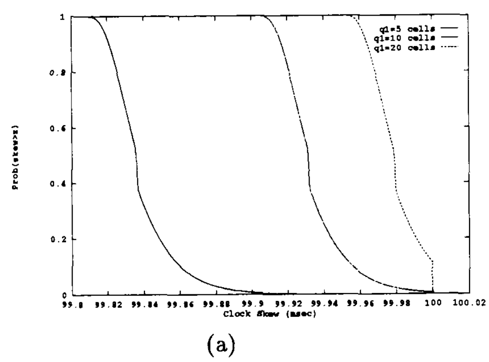

(a)

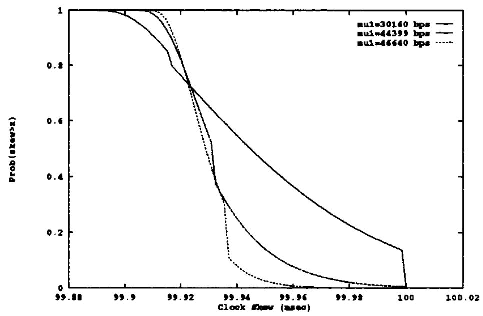

(b)

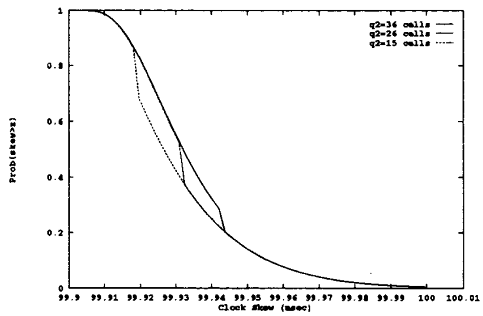

(c)

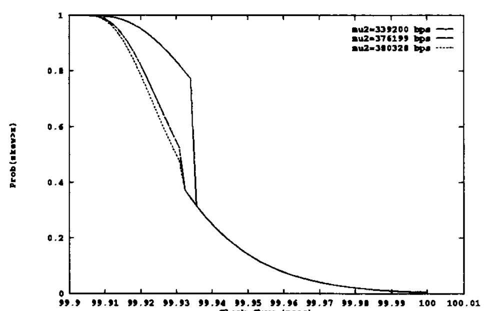

(d)

Figure 5: Probability distributions of clock skew at synchronization point with different allocation of (a) q_1, (b) μ_1, (c) q_2 and (d) μ_2

quite significant impact on the clock skew distribution. We can also see from the figures that the amount of resources allocated to VC_1 has a dominating effect on the distribution of clock skew, because VC_1 has a much higher delay jitter which consequently contributes more to the accuracy of synchronization algorithm.

5 Conclusion

In this paper we develop a practical clock synchronization scheme which only requires a minimal number of communication messages. In our scheme the MT need not be synchronized with the MASes, and it needs only simple computation to determine the time skew of the MASes. We show that the maximum time interval between mutual synchronization of clocks is mainly determined by the clock drift rate and the permissible time skew. We further show that time skew of the clocks of the media servers is significantly affected by the jitter of network delay. Our results show that the queuing delay of ATM switches can have a significant impact on the time skew of the clocks of the MASes. Therefore, the transmission delay, cell loss probability and the synchronization of clocks are equally important factors that should be considered in the allocation of network resources to virtual channels.

References

[1] C. Nicolaou, "An architechure for real-time multimedia communication system," *IEEE J. Select. Areas Commun.*, vol. 8, no. 3, pp. 391–400, March 1990.

[2] T. D. C. Little and A. Ghafoor, "Spatio-temporal composition of distributed multimedia objects for value-added networks," *IEEE Computers*, vol. 24, no. 10, pp. 42–50, Oct. 1991.

[3] D. P. Anderson and G. Homsy, "A continuous media I/O server and its synchronization mechanism," *IEEE Computers*, vol. 24, no. 10, pp. 51–57, Oct. 1991.

[4] S. Ramanathan and P. V. Rangan, "Adaptive feedback techniques for synchronized multimedia retrival over integrated networks," *IEEE/ACM Trans. on Networks*, vol. 1, no. 2, pp. 246–260, March 1993.

[5] T. D. C. Little and A. Ghafoor, "Multimedia synchronization protocols for broadband integrated services," *IEEE J. Select. Areas Commun.*, vol. 9, no. 9, pp. 1368–1482, Dec. 1991.

[6] S. R. Ahuja and J. R. Ensor, "Coordination and control of multimedia conferencing," *IEEE Commun. Magzine*, vol. 30, no. 5, pp. 38–43, April 1992.

[7] J. S. Turner, "New directions in communications (or Which way to the information age?)," *IEEE Communications Magzine*, vol. 25, no. 10, pp. 8–15, 1986.

[8] G. M. Wooddruff, R. G. H. Rogers, and P. S. Richards, "A congestion control framework for high-speed integrated packetized transport," *GLOBECOM 88*, pp. 7.1.1–7.1.5, 1988.

[9] J. Y. Hui, "Resource allocation for broadband networks," *IEEE J. on Selected Areas in Communications*, vol. 6, no. 9, pp. 1598–1608, 1988.

[10] A. E. Eckberg, Jr., D. T. Luan, and D. M. Lucantoni, "Meeting the challenge: Congestion and flow control strategies for broadband information transport," *Proc. IEEE GLOBECOM'89*, pp. 1769–1773, 1989.

[11] M. Hirano and N. Watanabe, "Characteristics of a cell multiplexer for bursty ATM traffic," *Proc. IEEE ICC'89*, pp. 399–403, 1989.

[12] G. Gallassi, G. Rigolio, and L. Fratta, "ATM: Bandwidth assignment and bandwidth enforcement policies," *Proc. IEEE GLOBECOM'89*, 1989.

[13] A. Gersht and K. J. Lee, "A congestion control framework for ATM networks," *IEEE J. Selected Areas on Communications*, vol. 9, no. 7, pp. 1119–1130, 1991.

[14] T. Murase, H. Suzuki, S. Sato, and T. Takeuchi, "A call admission control scheme for ATM network using a simple quality estimate," *IEEE J. on Selected areas in Communications*, vol. 9, no. 9, pp. 1461–1470, Dec. 1991.

[15] H. Saito, "Call admission control in an ATM network using upper bound of cell loss probability," *IEEE Trans. on Communications*, vol. COM-40, no. 9, pp. 1512–1521, Sept. 1992.

[16] Y. Hao and J. C. Liu, "A average-renewal-cycle-based admission control scheme in ATM networks," *submitted for publication*, 1993.

[17] L. Zhang, "A new architechture for packet switching network protocols," Technical report, Ph. D. Thesis, Dept. of Electrical Eng. and Computer Sci.,MIT, August 1989.

[18] S. J. Golestani, "Congestion-free transmission of real-time traffic in packet networks," *INFOCOM-90*, pp. 527–536, 1990.

[19] F. Guillemin, P. Boyer, A. Dupuis, and L. Romoeuf, "Peak rate enforcement in ATM networks," *Proc. IEEE INFOCOM'92*, pp. 753–758, 1992.

[20] J. J. Bae and T. Suda, "Survey of traffic control schemes and protocols in ATM networks," *Proceedings of the IEEE*, vol. 79, no. 2, pp. 170–189, Feb. 1991.

[21] L. Dittmann and S. B. Jacobsen, "Statical multiplexing of identical bursty sources in as ATM network," *Proc. IEEE GLOBECOM'88*, vol. 5, no. 6.5, pp. 39.6.1–39.6.5, 1988.

[22] Y. Hao and J. C. Liu, "An effective burst-level adaptive resource management scheme in ATM networks," Technical report, Dept. of Computer Science, Texas A&M University, 1993.

[23] R. Guerin, H. Ahmadi, and M. Naghshineh, "Equivalent capacity and its application to bandwidth allocation in high-speed networks," *IEEE J. on Selected Areas in Communications*, vol. 9, no. 7, pp. 968–981, 1991.